



substances can enter dearomatization pathways. At the certain choice of veratric acid concentration and cell density, oscillations of methoxyphenolic compounds can be observed in bacterial culture [3, 4]. In order to explain observed oscillations we have proposed a kinetic model of a cycle of four methylation-demethylation reactions [5, 6]. As a dynamical system, this model had some analogies to neurone oscillator proposed by Dunin-Barkovsky [7]. The model was highly asymmetrical because of the two following assumptions. 1. We treated veratric acid as a reservoir substance and its concentrations as a parameter of the system. 2. The ratio of the rate constants for methylation and demethylation reactions could be essentially different from unity. It had one or three equilibrium points depending on parameters values. When there was one equilibrium point, the system relaxed to the stable equilibrium or oscillated around the unstable equilibrium. At three equilibrium points the system behaved as a bistable trigger or as an excitable system.

Most of these features are conserved also in a more symmetrical system. In this paper I consider a model in which the only source of asymmetry are essentially different rate constants of forward and backward reactions. Consideration of this kind of model appeared to be necessary for an analysis of synchronisation of the processes taking place in different bacterial cells in a culture.

#### FORMULATION AND GENERAL PROPERTIES OF THE MODEL

The basic structure of the system (Fig. 1) is the same as that presented in previous paper [5]. Veratric acid (Fig. 1b) added to the culture of bacteria *Rhodococcus erythropolis* is demethylated two times to give protocatechuic acid (Fig 1c). Conversions  $a \leftrightarrow x$  and  $z \leftrightarrow y$  in Fig. 1a correspond to demethylation-methylation reactions at the position 4. In a similar way, conversions  $x \leftrightarrow y$  and  $a \leftrightarrow z$  correspond to the same reactions at the position 3.

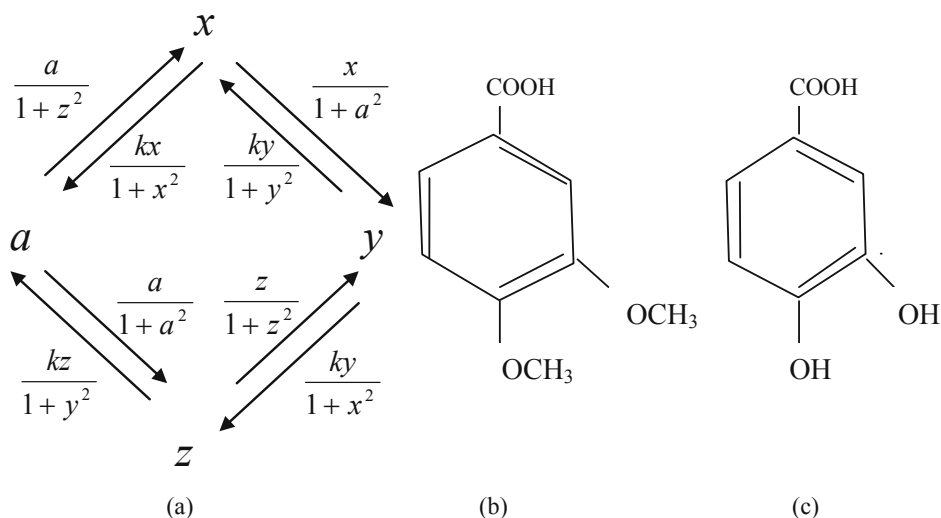


**FIG. 1.** (a) The cycle of reactions. Expressions next to the arrows describe the rates of respective reactions, *a* represents veratric acid (b), *x* and *z* isomers of vanilic acid and *y* protocatechuic acid (c).

At the arrows in Fig. 1a there are given expressions relating the rates of corresponding reactions to the concentrations of reagents. These relations are based on the following assumptions:

1. Veratric acid (*a*) acts as a corepressor of the 3-O-demethylase.
2. Vanilic acid (*x*) acts as a corepressor of the 4-methylase.
3. Protocatechuic acid (*y*) acts as a corepressor of the 3-methylase.
4. Isovanilic acid acts as a corepressor of the 4-O-demethylase.

Following other authors [8-13], we use the expression  $1/(1+r^m)$  with  $m=2$  to describe the influence of the corepressor concentration on the concentration of the corresponding enzyme. More detailed discussion of this question have been presented earlier [5]. Kinetic relations shown in Fig. 1a can alternatively describe allosteric inhibition of enzymes instead of their repression. The scheme in Fig. 1a can be also related to reversible substitution reactions in two different positions in some other molecules, not necessary in veratric acid.

Under these assumptions, the evolution of the system can be described by the following set of ordinary differential equations:

$$\frac{da}{dt} = \frac{-a}{1+a^2} + \frac{kx}{1+x^2} + \frac{kz}{1+y^2} - \frac{a}{1+z^2}, \quad (1)$$

$$\frac{dx}{dt} = \frac{-x}{1+a^2} - \frac{kx}{1+x^2} + \frac{ky}{1+y^2} + \frac{a}{1+z^2}, \quad (2)$$

$$\frac{dy}{dt} = \frac{x}{1+a^2} - \frac{ky}{1+x^2} - \frac{ky}{1+y^2} + \frac{z}{1+z^2}, \quad (3)$$

$$\frac{dz}{dt} = \frac{a}{1+a^2} + \frac{ky}{1+x^2} - \frac{kz}{1+y^2} - \frac{z}{1+z^2}. \quad (4)$$

Equations (1-4) describe the same set of reactions as that analysed earlier [5]. This time, however, we treat veratric acid concentration ( $a$ ) as a dynamical variable and not as a constant parameter. The dynamical system (1-4) is positively invariant and satisfies the microequilibrium postulate. Proofs of the both properties given in the earlier paper [5] remain valid. It follows from equations (1-4) that

$$\frac{d}{dt}(a+x+y+z) = 0. \quad (5)$$

So, there is an integral of motion

$$a+x+y+z = C = \text{const.} \quad (6)$$

It means that the sum of concentrations of all reagents is conserved. In fact, the system could be treated as the system of the order three. One dynamical variable could be eliminated using the conservation law (6). However, highly symmetrical shape of the equations (1-4) is more convenient for calculation than the corresponding system of the third order. The system (1-4) has one useful property. The substitution:

$$a \rightarrow y, \quad x \rightarrow z, \quad y \rightarrow a, \quad z \rightarrow x, \quad k \rightarrow 1/k \quad (7)$$

into equations (1-4) and rescaling the time according to the relation:

$$t' = \frac{t}{k} \quad (8)$$

results in the set of equations which is identical with the starting one. So, at the same value of  $C$ , the systems with relative rate constants  $k$  and  $1/k$  have the same number of equilibrium points with the same stability properties. Even more, the following relations between solutions of both systems take place:

$$a_1(t)=y_2(t/k), \quad x_1(t)=z_2(t/k), \quad y_1(t)=a_2(t/k), \quad z_1(t)=x_2(t/k), \quad (9)$$

where subindex 1 and 2 refer to solutions with relative rate constants  $k$  and  $1/k$  respectively. Of course, relations (9) will be valid if initial conditions satisfy relations (7). Evolution of the system depends on the values of parameter  $k$  and integral of motion  $C$ . In Fig. 2 there are shown two areas A and B, marked with double horizontal lines, where the system has three equilibrium points. In the area A there are two stable equilibrium points separated by the third unstable equilibrium (saddle point). At  $k$  and  $C$  belonging to this area, the system behaves as a bistable trigger. In the area B the system has the following equilibrium points: stable node, saddle-point and unstable focus. At values  $k$  and  $C$  from the area B, the system behaves as an excitable system.

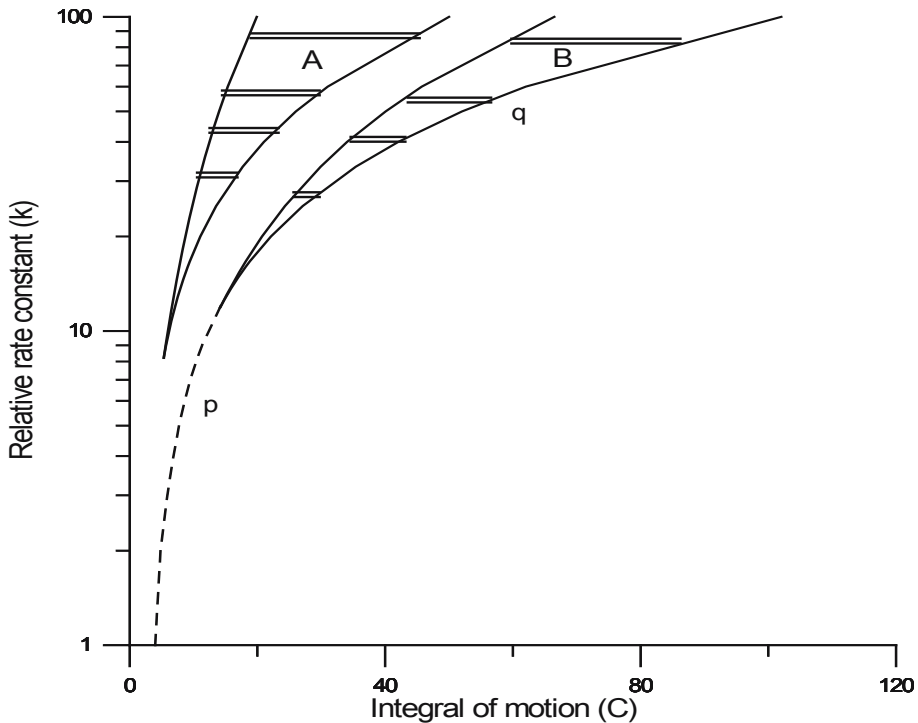


**FIG. 2.** Parameter plane of the system. The system has two stable and one unstable equilibrium points in the area A, one stable and two unstable equilibrium points or three unstable equilibrium points in the area B. Beyond the areas A and B the system has one equilibrium. Curve p separates areas with one stable equilibrium point from that with no stable equilibrium point. Curve q separates the area B with three equilibrium points from that with single equilibrium. The curves are based on numerically calculated equilibrium points using “Mathematica” with machine precision (16 digits) and printing of six significant decimal digits. For more details see text.

An exemplary phase portrait of this kind is shown in Fig. 6. There is a very narrow part of the area B at its right-hand edge, where all three equilibrium points are unstable. In this case, the autooscillations appear in the system. Beyond the areas A and B the system has one equilibrium point. The single equilibrium is stable for values of  $C$  smaller than those falling in the curve  $p$  in Fig. 2, and is unstable for the higher values of  $C$ . All the mentioned areas, shown for  $k > 1$  in Fig. 2, appear also at  $k < 1$ . Corresponding curves dividing the parameter plane at  $k < 1$  are symmetrical on the logarithmic scale of  $k$  to those shown in Fig. 2 in respect to the straight line  $k = 1$ . The borders of the areas shown in Fig. 2. have been determined numerically with the precision of six significant decimal digits.

## EVOLUTION OF THE SYSTEM

### AUTOOSCILLATIONS

Autooscillations appear in the system at the values of  $C$  higher than those corresponding to the curve  $p$  in Fig. 2. Inside the area B the curve  $p$  goes slightly above the curve  $q$ . So, there is a narrow strip of the area B between  $p$  and  $q$  where the system has three unstable equilibrium points. For parameter values belonging to this strip, the system has oscillatory solutions with all three equilibrium points placed inside the corresponding limit cycle.

Analytical linear analysis of stability is possible only in the fully symmetrical case with  $k = 1$ . In this case the system has an unique equilibrium

$$a = x = y = z = \frac{C}{4}. \quad (10)$$

Eigenvalues of the system in the vicinity of the equilibrium point (10) are given by the expressions (11):

$$\lambda_{1,2} = 32 \left[ \frac{C^2 - 16}{(16 + C^2)^2} \pm i2C^2 \right], \quad \lambda_3 = \frac{-4}{1 + a^2}, \quad (11)$$

The fourth eigenvalue is equal to zero. Respective normal variables can be defined by the transformation (12). Because of the conservation law (6) the variable  $\xi_4$  has a constant value  $C/2$ , and the evolution of the system can be represented in a 3-dimensional space  $(\xi_1, \xi_2, \xi_3)$ .

$$\begin{bmatrix} \xi_1 \\ \xi_2 \\ \xi_3 \\ \xi_4 \end{bmatrix} = \begin{bmatrix} \frac{1}{\sqrt{2}} & 0 & \frac{-1}{\sqrt{2}} & 0 \\ 0 & \frac{1}{\sqrt{2}} & 0 & \frac{-1}{\sqrt{2}} \\ \frac{1}{2} & \frac{-1}{2} & \frac{1}{2} & \frac{-1}{2} \\ \frac{1}{2} & \frac{1}{2} & \frac{1}{2} & \frac{1}{2} \end{bmatrix} \begin{bmatrix} a \\ x \\ y \\ z \end{bmatrix}. \quad (12)$$

Numerical solutions  $a(t)$  at  $k=1$  and  $C=5$  or  $50$  are shown in Fig. 3. Solutions  $x(t)$ ,  $y(t)$  and  $z(t)$  have the same shape as  $a(t)$  but are delayed in respect to  $a(t)$  by one, two and three quarters of the period respectively. The period of oscillations increases with growing values of  $C$  (see Fig. 4).

At values of  $k$  essentially different from the unity, the shapes of oscillations of variables  $a$ ,  $x$ ,  $y$  and  $z$  became different from each other. As an example, solutions  $a(t)$ ,  $x(t)$ ,  $y(t)$  and  $z(t)$  at  $k=40$  and initial conditions  $a(0)=80$ ,  $x(0)=y(0)=z(0)=0$  are shown in Fig. 5. According to the substitution (9), solutions for  $k=1/40=0.025$  and initial conditions  $y(0)=80$ ,  $a(0)=x(0)=z(0)=0$  can be obtained from Fig. 5. It is enough to change the time scale by substitution 2000 instead of 50 for the highest value of time and read Fig. 5a as  $y(t)$ , 5b as  $z(t)$ , 5c as  $a(t)$  and 5d as  $x(t)$ . Dependence of the oscillation period on the sum of reagent concentrations for a few values of  $k$  is shown in Fig. 4. The curves presented in Fig. 4 were obtained on the basis of numerical solutions of equations (1-4). Let us note that at high values of  $k$  the period of oscillations remains almost constant in a quite wide range of  $C$ . For example, at  $k=20$  the period changes its value from 9.60 at  $C=40$  to 10.16 at  $C=100$ . So, at such values of  $k$  the system can work as a pacemaker for some rhythms.

#### EVOLUTION OF THE SYSTEM AT MULTIPLE EQUILIBRIUM POINTS

At sufficiently high values of  $k$  the system can have three equilibrium points (areas A and B in Fig. 2). In the area A, at  $k > 8.2068$ , two of these equilibrium points are stable and the third one is unstable. Let us consider, as an example, the system with  $k=40$ . At this value of  $k$ , the area A includes the range of  $C$  from 12.4932 to 21.0277. The values of the variables in equilibrium and corresponding eigenvalues for  $k=40$  and  $C=16.6$  are given in Table 1. The dynamical variables in the unstable equilibrium (point 2 in Table 1) have intermediate values in respect to those describing the two stable equilibrium points. Thus, in the state space of the system, the unstable equilibrium point is situated somewhere between the stable equilibrium points. Depending on initial conditions, the system goes to the equilibrium 1 with relatively low value of  $x$

or to the equilibrium 3 with a high value of  $x$ . The equilibrium points 2 and 3 become closer and closer to each other when the value of  $C$  decreases from 16.6 to 12.5. At the same time the domain of attraction of the equilibrium 1 is growing. Eventually, at  $C=12.4932$ , the equilibrium points 2 and 3 annihilate. In contrast, increasing value of  $C$  from 16.6 to 21 brings the equilibrium points 1 and 2 closer and closer to each other. These equilibrium points annihilate at  $C=21.0277$ . I did not explore in detail the hypersurface separating attraction domains of the equilibrium points 1 and 3. Nevertheless, it is intuitively clear that the attraction domain of the equilibrium with a low value of  $x$  (point 1 in Table 1) is bigger at the left-hand edge of the area A (Fig. 2) than at the right-hand edge of this area. In the whole area A in all of the three equilibrium points, the values of  $y$  and  $z$  constitute only a minute part of the pool of all reagents ( $C$ ). Fully analogical discussion can be applied to the area with  $k < 1/8.2068 = 0.0840336$  with respective changes in the roles of variables and scale of time, according to the substitutions (7) and (8). There is another area (B in Fig. 2) with three equilibrium points. This area appears at  $k > 11.9$  or at  $k < 1/11.9 = 0.0840336$ .

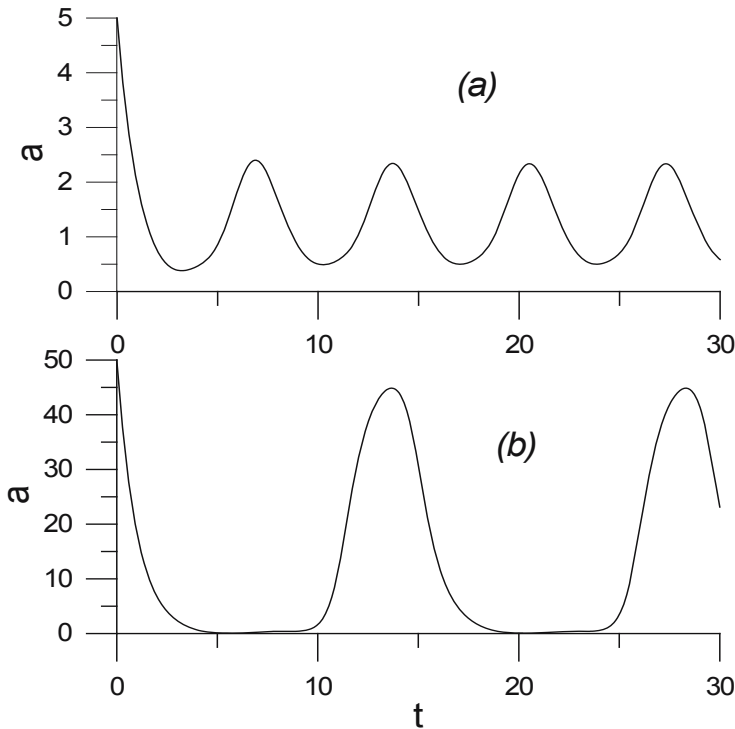


**FIG. 3.** Oscillations in a fully symmetrical system. Numerical solutions  $a(t)$  at  $k=1$  and  $C=5$  (a) or  $C=50$  (b).



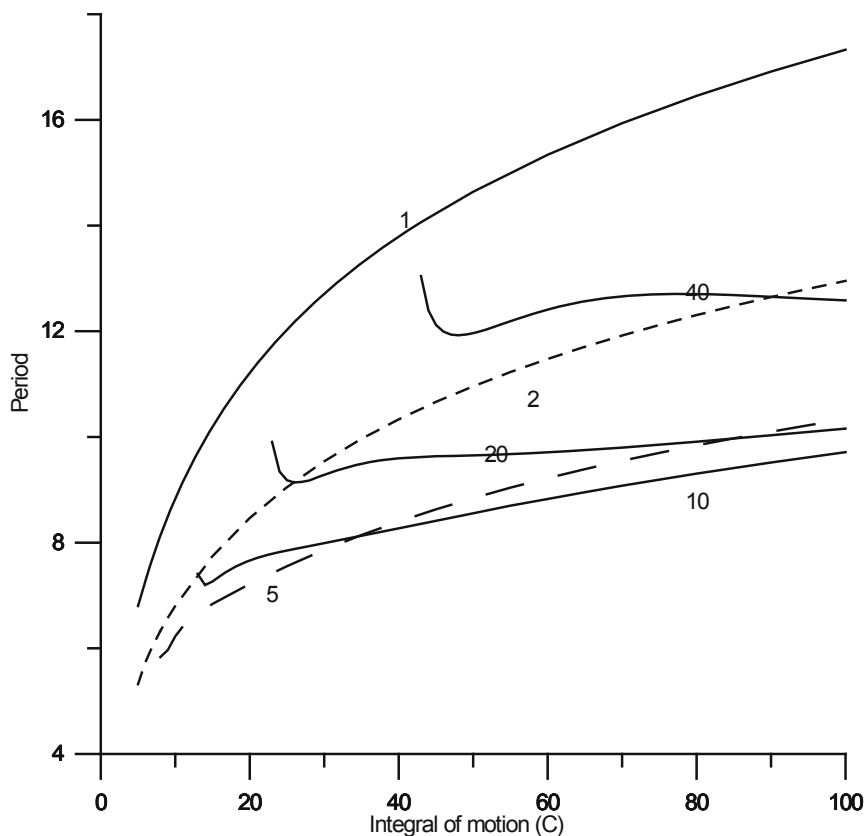


**FIG. 4.** Dependence of the period of oscillations on the sum of reagent concentrations ( $C$ ). Values of the relative rate constant  $k$  are shown at the respective curves. Periods were obtained from numerical solutions of equations (1-4), using “Mathematica”.

Let us return to the example with  $k=40$ . For this value of  $k$  and  $C$  belonging to the interval  $(21.0277, 34.1035)$ , the system has a single stable equilibrium characterised by three real and negative eigenvalues. As soon as  $C$  exceeds the value of 34.1035, two additional equilibrium points appear. Both of them are unstable. The system has three equilibrium points for  $34.1035 < C < 42.0551$ . Table 2 presents an example of such three equilibria for  $C=38$ . As can be seen from Table 2, the saddle-point (2) is located between the stable node (1) and unstable focus (3). In any case, the evolution of the system leads to equilibrium 1. However, orbits attaining equilibrium 1 can be essentially different for different initial conditions. In Fig. 6, there are shown projections of the two orbits on the plane  $(a, x)$  for the values of  $k=40$  and  $C=38$  as those used in Table 2. In the case of the orbit starting from the point A (initial conditions  $\{a(0), x(0), y(0), z(0)\} = \{1.134, 35.4, 1.408, 0.058\}$ ) changes in the values of the variables are very small. The system relaxes to equilibrium 1 almost monotonously. In contrast, on the orbit

starting from point B ( $\{a(0), x(0), y(0), z(0)\}=\{1.66, 30.63, 5.33, 0.38\}$ ) the amplitudes of changes of the variables are much higher. Before attaining equilibrium 1, the orbit goes around the unstable equilibrium 3. So, we have to do with an excitable system. Excitation events are somewhat different from those described earlier [5]. Generation of positive spikes of all variables in the present system is impossible because of the conservation law (6). After start from the point B, one can observe diminishing value of  $x$ , which reaches its minimum of 21.74 at time 3.6. In expense of  $x$ , spikes of the remaining variables are generated. The maximum values appear in the following sequence:  $y(2.97)=12.35$ ,  $z(4.31)=1.72$  and  $a(5.61)=4.92$ . Even minimum value of  $x$  is essentially higher than maximum values of  $y$ ,  $z$  and  $a$ .

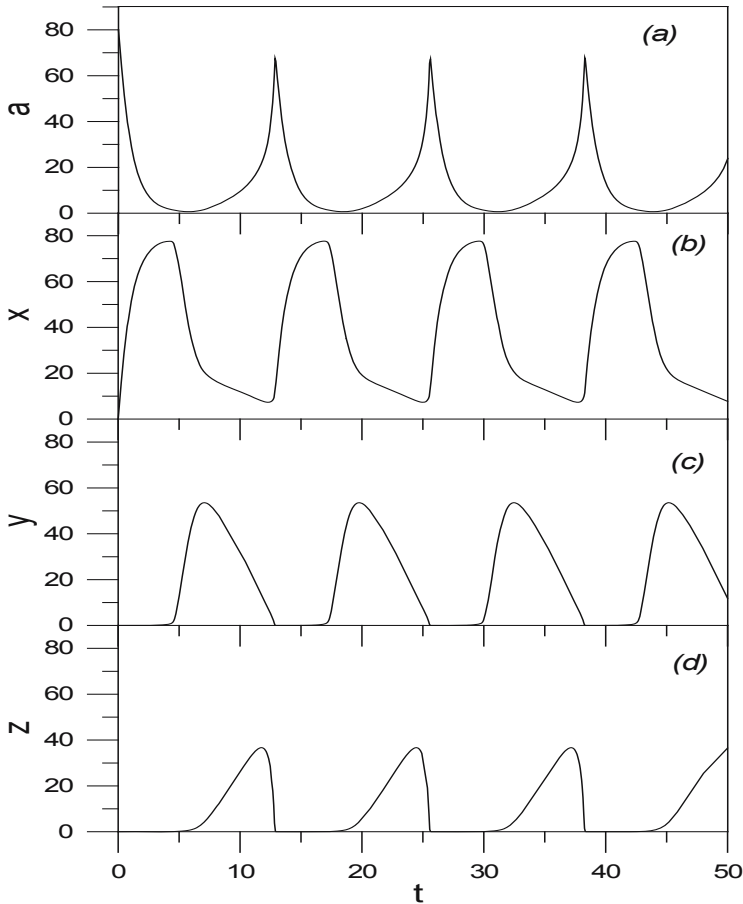


**FIG. 5.** Oscillations in a highly asymmetrical system. Numerical solutions at  $k=40$  and  $C=80$ .

**TABLE 1.** Coordinates  $(a,x,y,z)$  and respective eigenvalues  $(\lambda)$  of the equilibrium points at  $k=40$  and  $C=16.6$ 

Equilibrium no.	1	2	3
$a$	16.0935	14.1969	2.9172
$x$	0.504903	2.40104	13.6393
$y$	$4.85482 \times 10^{-5}$	$2.96349 \times 10^{-4}$	$3.59011 \times 10^{-2}$
$z$	$1.54745 \times 10^{-3}$	$1.75225 \times 10^{-3}$	$7.67861 \times 10^{-3}$
$\lambda_1$	-72.8782	-46.9177	-41.2675
$\lambda_2$	-39.996	-39.9947	-39.7528
$\lambda_3$	-19.9246	3.16435	-0.798068

**TABLE 2.** Coordinates  $(a,x,y,z)$  and respective eigenvalues  $(\lambda)$  of the equilibrium points at  $k=40$  and  $C=38$ 

Equilibrium no.	1	2	3
$a$	1.09956	1.16751	2.16193
$x$	36.3598	34.4423	26.8251
$y$	0.524838	2.31183	8.34074
$z$	0.0158716	0.0783655	0.67221
$\lambda_1$	-32.844	-7.75538	-1.48735
$\lambda_2$	-17.7117	-0.731001	$0.230103+0.829406i$
$\lambda_3$	-1.02994	4.1651	$0.230103-0.829406i$

The variable  $x$  constitutes also a dominating fraction of the whole reagent pool in all equilibrium points (see Table 2). So, in the excitable regime (area B in Fig. 2), the variable  $x$  behaves like a reservoir substance. Coordinates of the saddle-point 2 determine the excitation threshold. The value of  $C=38$  used in Table 2 and Fig. 6 corresponds to the middle of the area B in Fig. 2 at  $k=40$ . At the left-hand edge of this area, at  $C$  slightly higher than 34.1035, the saddle-point 2 and unstable focus 3 are very close each to other and both are remote from stable node 1. In such a situation the excitation threshold is relatively high and amplitudes of generated spikes of the variables are relatively low. With the growing value of  $C$  equilibrium points 1 and 2 come closer and closer to each other. The excitation threshold becomes lower and lower. At  $C=42.0548$ , still inside the area B in Fig. 2, destabilisation of the equilibrium 1 takes place. So, in the interval  $42.0548 < C < 42.0551$  the system has three unstable equilibrium points and oscillative solutions. At  $C=42.0551$  the equilibrium points 1 and 2 annihilate. Again, analogical discussion can be applied to  $k=1/40=0.025$  with substitution (7). All processes will then be 40 times slower according to time rescaling (8).

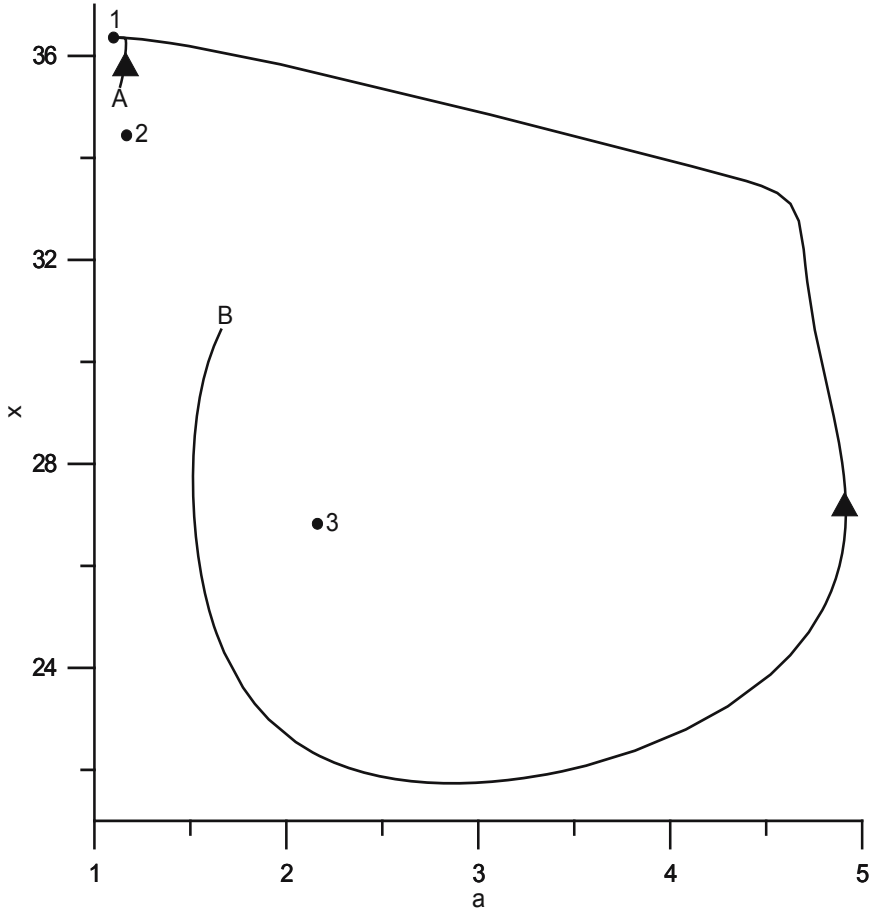


**FIG. 6.** Excitable system. Projections of the two orbits on the plane  $(a,x)$  at  $k=40$  and  $C=38$ . Coordinates of stable node (1), saddle-point (2) and unstable focus (3) are given in Table 2. Orbit starting from the point A (1.134, 35.4, 1.408, 0.058) corresponds to subthreshold relaxation. Orbit starting from the point B (1.66, 30.63, 5.33, 0.38) corresponds to excitation. Orbits obtained from numerical solutions of the equations (1-4) using “Mathematica”.

## CONCLUSIONS

The dynamical system (1-4) shares many modes of evolution with one analysed earlier [5]. Providing a proper choice of parameter values, both systems can relax to an unique stable equilibrium or behave as bistable triggers. Both

systems can have autooscillatory solutions and can behave as excitable systems. But in contrast to the earlier presented system with one reservoir substance, the system (1-4) can not behave as a transducer of stimulus strength to frequency. Both systems can describe metabolic oscillations in a single bacterial cell. Such oscillations will appear in a bacterial culture if oscillations in different cells are synchronous. I suppose that both considered systems will be useful in searching favourable conditions for synchronisation.

## REFERENCES

1. Malarczyk, E. (1989) *Transformations of phenolic acids by Nocardia*. Acta Microbiol. Polon. **38**, 45-53.
2. Malarczyk, E. and Kochmańska-Rdest, J. (1990) *New aspects of co-regulation of decarboxylation and demethylation activities in Nocardia*. Acta Biochim. Polon. **34**, 145-148.
3. Malarczyk, E. and Paździoch-Czochra, M. (2000) *Multiple respiratory bursts as a response to veratrate stress in Rhodococcus erythropolis*. Cell Biol. Int. **24**, 515-527.
4. Paździoch-Czochra, M., Malarczyk, E. and Siewiesiuk, J. (2003) *Relationship of demethylation processes and cell density in cultures of Rhodococcus erythropolis*. Cell Biol. Int. **27**, 325-336.
5. Siewiesiuk, J. and Malarczyk, E. (2002) *A cycle of enzymatic reactions that behaves as a neuronal circuit*. J. Theor. Biol. **214**, 255-262.
6. Siewiesiuk, J., Czubla, A., Malarczyk, E. and Paździoch, M. (1999) *Kinetic model for oscillations in a cycle of enzymatic reactions related to methoxyphenol transformation in Rhodococcus erythropolis culture*. Cell. Mol. Biol. Lett. **4**, 131-146.
7. Dunin-Barkovsky, V.L. (1970) *The oscillation of activity level in simple closed neurone chains*. Biophysics **15**, 374-378 (in Russian).
8. Goodwin, B.C. (1966) *An entrainment model for timed enzyme syntheses in bacteria*. Nature **209**, 479-481.
9. Hastings, S., Tyson, J. and Webster, D. (1977) *Existence of periodic solutions for negative feedback cellular control systems*. J. Differential Equations **25**, 39-64.
10. Tyson, J.J. (1975) *On the existence of oscillatory solutions in negative feedback cellular control processes*. J. Math. Biol. **1**, 311-315.
11. Tyson, J.J. (1979) *Periodic enzyme synthesis: reconsideration of the theory of oscillatory repression*. J. Theor. Biol. **80**, 27-38.
12. Grigorov, N.L., Poljakova, M.S. and Chernavsky, D.S. (1967) *Model investigations of the trigger schemes and the differentiation process*. Molecular Biol. **1**, 410-418, (in Russian).
13. Romanovsky, Yu.M., Stepanova, N.V. and Chernavsky, D.S. (1975) *Mathematical Modelling in Biophysics*, Nauka, Moscow.